CRATERING ON PLANETARY BODIES DUE TO SPACECRAFT LANDINGS. M. Mehta[1], N. O. Renno[1], A. Sengupta[2], M. Pokora[1] [1]University of Michigan, 2455 Hayward St., Ann Arbor, MI 48109, [2]NASA Jet Propulsion Laboratory, California Institute of Technology, Pasadena, CA 91109. manishm@umich.edu, renno@alum.mit.edu, anita.sengupta@jpl.nasa.gov, mpokora@umich.edu

Introduction: Spacecraft landings on planetary bodies provides important information to both planetary science and engineering. The craters developed by supersonic exhaust plumes from descent rocket motors can provide approximations to the bulk soil properties, predict altered ground morphology, landing site contamination, and determine the erosion physics at these extreme conditions. The understanding of these interactions is also important for mission planning and risk reduction [1]. This article briefly investigates the plume flow fields and the cratering mechanisms caused by jet impingement on various planetary surfaces, and describe their implications to science and engineering.

Rocket plume flow field: The exhaust plume's shock structure and dynamics determine the nature of erosion. The flow fields and impingement pressure are dependent on the jet expansion ratio (e), the pressure ratio between the exhaust plume at the nozzle exit and planetary atmosphere (Fig.1). Plemmons *et al.* [2] showed that pulsed jets at Mars atmospheric conditions produce much larger ground pressure perturbations than steady jets. Jet flow fields have three regimes: over-expanded ($e < 1$); perfectly expanded ($e = 1$) and underexpanded ($e > 1$) [2]. Numerical and experimental simulations indicate that highly over-expanded jets in the terrestrial atmosphere develop oblique and normal shock waves in the nozzle, and that shear instabilities at the jet boundaries and shock wave instabilities accelerate plume decay. This results in the rapid transition to subsonic turbulent jets and modest normalized ground pressure values (normalized by total pressure at the thruster inlet chamber, Pc) (Fig. 1). Land and Scholl showed that highly under-expanded jets in the lunar atmosphere results in shockwave expansion [3] which causes the jet impact loads to be distributed over a large area and therefore to have modest pressure magnitudes (Fig. 1). Exhaust plumes in the martian atmosphere are compact and collimated and hence possess the highest ground pressure values among the cases that we studied (Fig. 1). We show that these jets have supersonic core lengths greater than 35 nozzle exit diameters (d) as opposed to highly over-expanded jets which are less than $5d$ (Fig. 1). The plume structure dynamics and ground pressure values directly affect the cratering mechanisms.

Cratering: The most prevalent cratering mechanism during spacecraft landings has been viscous shear erosion (VSE) as observed for the NASA Apollo, Surveyor and Viking missions. This occurs for relatively low ground pressure values when the shear stress forces caused by the jet exceed the cohesive and friction forces of the granular medium. Fig. 2b shows the characteristic erosion rate profile, erosion rate vs. densimetric Froude number (Fr), of VSE processes on planetary bodies. There is a semi-log linear rise in erosion rate (gravitational regime) to a maximum at Fr ~60 and then a linear decline (shear strength regime) to Fr ~1000. With decreasing Fr, the granular particle sizes increase which inhibits its' movement due to increase in particle weight. With increasing Fr, the particle sizes decreases which results in a linear decrease in erosion rates due to the development of interparticle cohesive forces (Fig. 2a). These curves were developed from landing site and experimental data [3,4].

Mehta *et al*. recently discovered a new erosion process named diffusive gas explosive erosion (DGEE) [5] due to pulsed underexpanded jets which does not obey this characteristic erosion rate curve for the range of Fr studied. DGEE only produces a linear semi-log increase in erosion rate with Fr (Fig. 2a). This may be attributed to local fluidization of the soil and granular shock wave propagation [5]. The fluidization breaks interparticle forces, separating the particles from one another, and hence, the erosion rate is mainly dependent on the pressure gradient and particle weight. Soil permeability and atmospheric pressure both affect the developing pressure gradient. As observed in Fig. 2, DGEE produces erosion rates many orders of magnitude larger than other jet-induced cratering mechanisms. Its erosion effects at the Phoenix landing site are shown in Fig. 3 and are compared to previous planetary missions (Table 1). Most importantly, DGEE led to the discovery of an extensively exposed water ice surface and liquid saline water at the Phoenix landing site (Fig. 3) [5,6]. Our new calculations show that this process exposed the subsurface ice over a radius of ~80 cm from the spacecraft centerline with a width of ~110 cm (Fig. 3a).

The third erosion process which may be important is bulk shear failure (BSF). This was observed on our recent experiments for NASA's 2011 Mars Science Lab Mission (MSL). This occurs when the impingement pressure of the jets exceeds the soil shear strength and forms steep parabolic craters that are partially redeposited after jet termination. The average erosion rate and final crater size are larger than those observed for VSE (Table 1). Experimental results also show that soil deposition may occur on the MSL deck.

Planetary science: Erosion rate characteristic curves (Fig. 2) provide information on soil particle size and cohesion. The erosion rate are averaged values from tests performed with dry martian soil simulant at depths between 5 and 20 cm, the range estimated at the Phoenix landing site [6]. These rates are normalized by the jet's mass flow rate. From Fig 2a, we estimate the soil cohesion present at the Phoenix landing site. The deviation from the characteristic curve suggests additional surface or external cohesion caused by a duricrust. External cohesive agents would show a decrease in normalized erosion rates for similar *Fr*. The external cohesion may be attributed to salts and pockets of brines within the regolith as observed by Renno *et al.* [6]. If we can quantify the cohesion present, these curves can more accurately determine the particle size, porosity and permeability at the landing site. More importantly, we may be able to assess the effect of brines on soil cohesion.

Conclusion: Exhaust plumes are collimated within the Mars atmospheric regime and thus demonstrate the largest ground pressure. DGEE can lead to extensive erosion of the landing site at martian environments. Not only did this mechanism lead to the first observation of liquid water at the Phoenix landing site, but erosion characteristic curves may provide further quantitative evidence for brines on Mars.

References: [1] Whetsel C. *et al.* (2000), NASA JPL D-18709. [2] Plemmons D.H. *et al.* (2008) *JGR,* 113, E00A11.[3] Land N.S and Scholl H.F. (1969) NASA TN-D 5051; [4] Romine G.L. *et al* (1973) NASA CR-2252. [5] Mehta M. *et al.* (2009) *Eos Trans. AGU*, 89, 53, Abs. #U11B-0028.[6] Renno N.O. *et al*. (2009) *JGR* 114, E00E03.

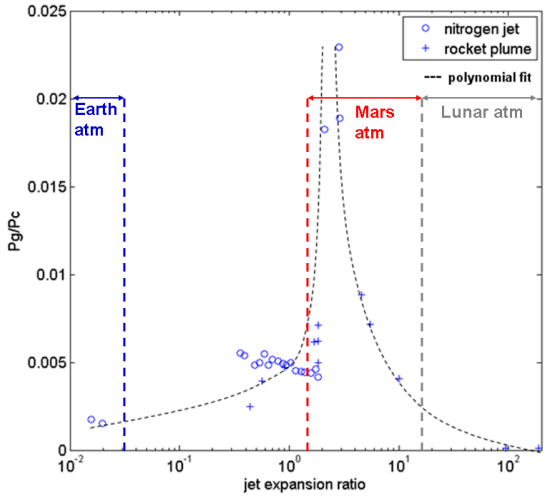

Fig. 1. Normalized plume impingement pressure vs. jet expansion ratio shown at three planetary environments: Earth, Mars and the Moon at a spacecraft altitude of ~35*d*.

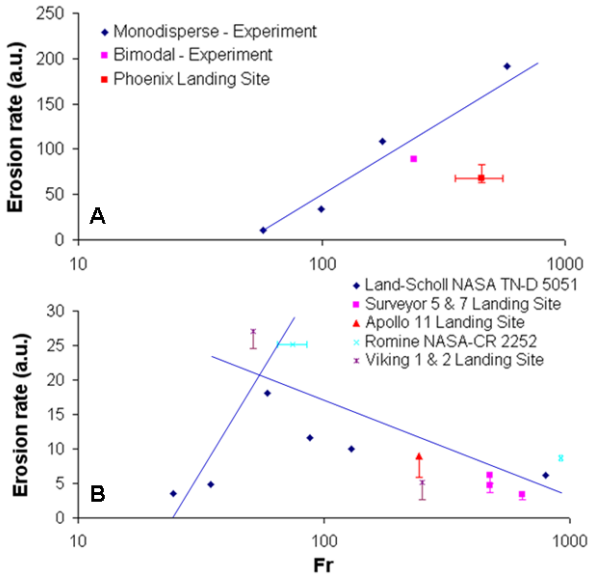

Fig. 2. Erosion rate characteristic curves of **(A)** DGEE and **(B)** VSE mechanisms.

TESTS	Max Erosion Depth (y/D)	Erosion Size (x/D)	Comments
APOLLO 11	< 0.01	0.6	Surface Scrubbing
SURVEYOR 5 & 7	< 0.12	~4.6 - 1.5	Surface Scrubbing
VIKING 1	~ 0.19 - 0.13	~2.5 - 1.9	10 cm x 20 cm cresent crater
VIKING 2	~ 0.25 - 0.19	~4.4 - 3.2	Three 6 cm diameter craters
PHOENIX	~0.79 - 0.47	~16.9 surf. erosion ~10.0/~8.4 exp	**Exposed ice**
Viking WSTF Test 1 Lunar Nominal	< 0.06	~0.0	No crater observed
Viking WSTF Test 2 Sand Dune	~0.22	~5	18 5 cm diameter craters
Phoenix Ames Test 1 160u sand	3.15	~18.7 - 14.7	Radial granular shocks
Phoenix Ames Test 2 160u/15u	~3.15 - 0.79	~13.1/~8.9 exp	Exposed surface; radial granular shocks
Phoenix Ames Test 3 <15u fines	3.15	>20.9/~11.6 exp	Exposed surface; radial granular shocks
Phoenix Ames Test 4 >1000u coarse sand	0.37	1.6	Minor erosion
MSL Ames Test 1 ~160u sand	< 0.50	~4.9	Bulk shear failure
Phoenix Ames Earth Test 1 160u sand (pulsed)	0.63	3.1	Parabolic crater
Phoenix Ames Earth Test 2 160u sand (steady)	1.02	2.9	Parabolic crater

exp-exposed; D – equivalent nozzle diameter

Table 1. Crater dimensions from landing site and simulation data at Lunar (grey), Mars (pink) and Earth (blue) environs.

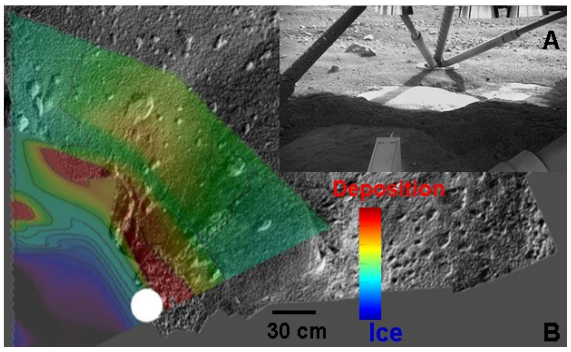

Fig. 3. (A) Crater/exposed ice under Phoenix **(B)** Topographical map of Phoenix work space.